Acta Pharmacologica Sinica

www.nature.com/aps

ARTICLE

The adipokine orosomucoid alleviates adipose tissue fibrosis via the AMPK pathway

Peng-yuan Wang[1], Jia-yi Feng[1], Zhen Zhang[1], Yi Chen[1], Zhen Qin[1], Xian-min Dai[1], Jie Wei[1], Bo-han Hu[1], Wei-dong Zhang[1], Yang Sun[1] and Xia Liu[1]

The excess deposition of underlying extracellular matrix (ECM) in adipose tissue is defined as adipose tissue fibrosis that is a major contributor to metabolic disorder such as obesity and type 2 diabetes. Anti-fibrosis therapy has received much attention in the treatment of metabolic disorders. Orosomucoid (ORM) is an acute-phase protein mainly produced by liver, which is also an adipokine. In this study, we investigated the effects of ORM on adipose tissue fibrosis and the potential mechanisms. We showed that ORM1-deficient mice exhibited an obese phenotype, manifested by excessive collagen deposition in adipose tissues and elevated expression of ECM regulators such as metalloproteinases (MMP-2, MMP-13, MMP-14) and tissue inhibitors of metalloproteinases (TIMP-1, TIMP-2, TIMP-3). Administration of exogenous ORM (50 mg· kg^{-1}· d^{-1}, ip) for 7 consecutive days in high-fat diet (HFD)-fed mice and leptin receptor (LepR)-deficient *db/db* mice attenuated these abnormal expressions. Meanwhile, ORM administration stimulated AMP-activated protein kinase (AMPK) phosphorylation and decreased transforming growth factor-β1 (TGF-β1) level in adipose tissues of the mice. In TGF-β1-treated 3T3-L1 fibroblasts, ORM (10 μg/mL) improved the impaired expression profiles of fibrosis-related genes, whereas a selective AMPK inhibitor dorsomorphin (1 μmol/mL) abolished these effects. Together, our results suggest that ORM exerts a direct anti-fibrosis effect in adipose tissue via AMPK activation. ORM is expected to become a novel target for the treatment of adipose tissue fibrosis.

Keywords: ORM; adipose tissue; fibrosis; AMPK; TGF-β1; 3T3-L1 fibroblasts; dorsomorphin; obesity; metabolic disorders

Acta Pharmacologica Sinica (2022) 43:367–375; https://doi.org/10.1038/s41401-021-00666-9

INTRODUCTION

Adipose cells are surrounded by extracellular matrix (ECM), which provides necessary support for adipose tissue. The balance between adipocytes and the ECM is of crucial importance for the normal function of adipose tissue [1, 2]. When obesity occurs, adipose tissue expands dynamically through adipocyte hypertrophy and/or hyperplasia, which leads to hypoxic conditions, as well as the continuous production and deposition of ECM. Excessive deposition of underlying pathological ECM is defined as adipose tissue fibrosis [1, 3–5]. Fibrosis can further impair the plasticity of adipocytes and exacerbate the formation of an anoxic microenvironment, leading to adipocyte death and adipose tissue dysfunction. There is substantial evidence that adipose tissue fibrosis is a major contributor to metabolic dysfunction, such as obesity and type 2 diabetes [6, 7] and is regarded as a hallmark of metabolic dysfunction in adipose tissue.

Studies have shown that the repression of adipose tissue fibrosis could improve systemic glucose homeostasis. For example, metformin is a first-line drug for treating obesity-related type 2 diabetes. Luo et al. found that metformin inhibited abnormal ECM remodeling and fibrosis in adipose tissue, improving insulin resistance in obesity by AMP-activated protein kinase (AMPK) in adipose tissue [8]. Hasegawa et al. found that GTF2IRD1, a cold-inducible transcription factor, repressed adipose tissue fibrosis and improved systemic glucose homeostasis through a PRDM16-EHMT1 complex [9]. Exercise training is also known to improve insulin resistance and type 2 diabetes mellitus. Recently, exercise was reported to attenuate adipose tissue fibrosis in diet-induced obese mice [10]. Currently, antifibrotic therapy targeting adipose tissue has received much attention in the treatment of metabolic diseases. However, the underlying mechanisms that regulate adipose tissue fibrosis remain largely unclear, which limit the development of antifibrotic drug discovery.

Orosomucoid (ORM), also known as α1-acid glycoprotein, is an acute-phase protein that is mainly produced in the liver. There are two isoforms of ORM (ORM1 and ORM2) in humans, one isoform (ORM) in rats, and three isoforms (ORM1, ORM2, and ORM3) in mice. Among them, ORM1 is the predominant isoform and the only isoform induced by acute-phase stimuli. ORM has a variety of biological activities, including immune modulation, drug delivery, and barrier maintenance [11, 12]. Recently, the role of ORM in extrahepatic tissues and organs, especially in adipose tissue, has drawn much attention. Specifically, ORM is induced in the adipose tissue of obese mice and is regulated in differentiated adipocytes by metabolic signals, including insulin, high glucose, and free fatty acids. Accordingly, ORM improved energy metabolism in adipocytes, as well as glucose and insulin tolerance in obese and diabetic *db/db* mice [13, 14]. Our previous studies also showed

[1]School of Pharmacy, Second Military Medical University/Naval Medical University, Shanghai 200433, China
Correspondence: Xia Liu (lxflying@aliyun.com) or Yang Sun (DawnySun@126.com) or Wei-dong Zhang (wdzhangy@hotmail.com)
These authors contributed equally: Peng-yuan Wang, Jia-yi Feng, Zhen Zhang

Received: 22 October 2020 Accepted: 22 March 2021
Published online: 19 April 2021

that in response to an acute or chronic nutritional state, ORM was significantly elevated in adipose tissue, the liver, and sera. Moreover, through hypothalamic LepR, ORM regulates food intake and energy homeostasis in a negative feedback loop [15], indicating that ORM is an important adipokine that regulates obesity and metabolism [13]. However, it remains unclear whether ORM is involved in the regulation of adipose tissue fibrosis.

In this study, we aimed to explore the direct role and potential mechanism of ORM in adipose tissue fibrosis. We found that ORM1-deficient mice exhibited fibrotic phenotypes in adipose tissue, while exogenous ORM activated AMPK and attenuated adipose fibrosis in vivo and in vitro. Thus, ORM was identified as a novel regulator of adipose tissue fibrosis.

MATERIALS AND METHODS

Animals

Eight-week-old male *db/db* mice and C57BL/6J mice were purchased from Changzhou Cavans Laboratory Animal Co., Ltd. Eight-week-old male C57BL/6J mice were fed a 60% high-fat diet (Changzhou SYSE Biotechnology Co., Ltd.) to induce the obese animal model. ORM (Sigma-Aldrich, 50 mg·kg^{-1}·d^{-1}) or vehicle was injected intraperitoneally for seven consecutive days, then mice were sacrificed, and adipose tissue was collected. ORM1-deficient mice were generated as previously described [16]. All animals were housed at 24 °C under a 12-h light–dark cycle. All animal experiments were performed in accordance with the National Institutes of Health Guide for the Care and Use of Laboratory Animals and with the approval of the Scientific Investigation Board of the Second Military Medical University.

Cell culture

3T3-L1 cells were purchased from the Cell Bank of the Chinese Academy of Sciences and cultured in high-glucose DMEM containing 10% FBS in an incubator at 37 °C with 5% CO_2. To establish a fibrosis model in vitro, 3T3-L1 cells (without inducing differentiation) in six-well plates were serum-starved in DMEM for 5 h and then exposed to transforming growth factor-β1 (TGF-β1) (5 ng/mL) for 24 h. For the drug treatment group, drugs (10-μg/mL ORM and/or 1 μmol/mL dorsomorphin) were added in combination with TGF-β1 and incubated for 24 h. Then, cells were harvested for further analysis.

Western blotting

Total protein was extracted, and immunoblotting was performed as described previously [15]. Briefly, tissues or cells were washed in PBS, homogenized and lysed in lysis buffer containing a protease inhibitor mixture (Kangchen, Shanghai, China). Protein concentrations were measured by a BCA protein assay kit (Beyotime, Shanghai, China). Proteins (30–50 μg) were separated by sodium dodecyl sulfate–polyacrylamide gel electrophoresis and transferred to a nitrocellulose membrane, which was then incubated with specific antibodies. Equal sample loading was confirmed by reprobing the blots for GAPDH or TUBULIN. The antibodies (1:1000, diluted in 1% BSA, 4 °C overnight) used were as follows: collagen I (ab34710, Abcam, Cambridge, MA, UK), collagen III (ab7778, Abcam, Cambridge, MA, UK), collagen VI (AF2740, Beyotime Biotechnology, Shanghai, China), TIMP-1 (bs-0415R, Bioss antibody Inc., Woburn, MA, USA), TIMP-2 (bs-0416R, Bioss antibody Inc., Woburn, MA, USA), TIMP-3 (bs-0417R, Bioss antibody Inc., Woburn, MA, USA), MMP-2 (bs-0412R, Bioss antibody Inc., Woburn, MA, USA), MMP-13 (bs-0575R, Bioss antibody Inc., Woburn, MA, USA), MMP-14 (bs-51028M, Bioss antibody Inc., Woburn, MA, USA), LOX (bs-15492R, Bioss antibody Inc., Woburn, MA, USA), α-smooth muscle actin (α-SMA) (bsm-33188M, Bioss antibody Inc., Woburn, MA, USA), TUBULIN (AT819–1, Beyotime Biotechnology, Shanghai, China), and GAPDH (AF5009, Beyotime Biotechnology, Shanghai, China). Images were obtained with an Odyssey infrared fluorescence imaging system (Li-Cor, Lincoln, NE, USA). The quantification of Western blot data was performed using ImageJ software (NIH, Bethesda, MD, USA).

RNA quantification

Total RNA was extracted from cells and tissues using Takara RNAiso plus. One thousand nanograms of each sample was reverse-transcribed to form cDNA using Takara PrimeScript RT master mix. Then, real-time PCR was performed using Roche Fast Start Universal SYBR Green master mix. The relative mRNA levels were normalized to the *Gapdh* mRNA levels, and the relative gene expression levels were determined with the $2^{-\Delta\Delta Ct}$ method. The primers were obtained from PrimerBank (https://pga.mgh.harvard.edu/primerbank/).

Magnetic resonance imaging (MRI)

MRI was used to assess the fat distribution and body composition of mice as previously reported [17] and was performed at Suzhou Niumag Analytical Instrument Corporation Shanghai Branch (Suzhou, China). At the end of the 21 weeks, the mice were weighed and placed directly in the NMR squirrel cage, and then body composition was measured using a small animal body composition analysis system (MesoMR23-60H; Niumag Electric Corporation, Shanghai, China) with a magnetic field strength of 0.5 T, frequency of 21.718 MHz, coil diameter of 60 mm, and magnetic temperature of 32 ± 0.01 °C. Body lean mass and body fat mass were calculated using the system software. Then, fat distribution in live mice was measured using a nuclear magnetic resonance (NMR) analyzer (MesoQMR23-060H-I; Niumag Electric Corporation, Shanghai, China) with a resonance frequency of 23.313 MHz, magnetic strength of 0.5 T, coil diameter of 40 mm, and magnetic temperature of 32 ± 0.01 °C. The mice were anesthetized and underwent coronal scanning with a layer thickness of 3.0 mm in the coronal plane. Then, MSE sequence data were acquired with the following experimental parameters: FOV read = 100 mm, FOV phase = 100 mm, TR = 360 ms, TE = 18.125 ms, slices = 6, slice width = 3 mm, slice gap = 0.5 mm, averages = 10, and K space = 192 × 256.

H&E and Masson's trichrome staining

Fresh adipose tissue was fixed in 4% paraformaldehyde for more than 24 h. Paraffin sections were prepared at a thickness of 4 μm. Then, hematoxylin and eosin (H&E) staining and Masson's trichrome staining were performed according to standard protocols using the adipose tissue slides. Photos were taken under an optical microscope (Olympus, Tokyo, Japan), and then adipocyte size and Masson's trichrome stain-positive areas were measured using ImageJ software (NIH, Bethesda, MD, USA).

Hydroxyproline level measurement

The hydroxyproline levels were measured using a hydroxyproline detection kit (D799573-0050) according to the manufacturer's instructions (Sangon Biotech, Shanghai, China).

Immunofluorescence staining

3T3-L1 cells were fixed with 4% PFA for 15 min, permeabilized with 0.5% Triton X-100 for 15 min at room temperature, and washed three times (5 min each time) with PBS. Nonspecific binding was blocked with 3% BSA at room temperature for 30 min. Cells were incubated with LOX (bs-15492R, Bioss antibody Inc., Woburn, MA, USA) and α-SMA primary antibodies (bsm-33188M, Bioss antibody Inc., Woburn, MA, USA) at 4 °C overnight, washed, incubated with Cy3-labeled goat anti-rabbit (A0516, Beyotime Biotechnology, Shanghai, China) and goat anti-mouse Alexa Fluor 488 secondary antibodies (A0568, Beyotime Biotechnology, Shanghai, China) for 30 min at room temperature. DAPI (C1006, Beyotime

Biotechnology, Shanghai, China) was used to visualize the cell nuclei. The slides were viewed and imaged with a Leica SP5 (Mannheim, Germany) confocal laser scanning microscope equipped with a ×63 objective. Three channels were used to acquire the images sequentially: the FITC laser (488 nm, green for α-SMA), the Cy3 laser (550 nm, red for LOX), and DAPI (405 nm, blue for nuclei). Quantification of the photomicrographs was performed by converting the images to grayscale, inverting the color and quantifying the field staining intensity with ImageJ software.

Statistical analysis

The data are presented as the mean ± SD. Statistical analyses were performed using GraphPad Prism. Two-tailed Student's *t* test was used for comparisons between two groups, and one-way ANOVA followed by Tukey's multiple comparison test was used for comparisons between more than two groups. $P < 0.05$ was considered statistically significant.

RESULTS

ORM1-deficient obese mice exhibit excessive collagen deposition

Our previous studies showed that ORM1-deficient mice exhibited significant increases in fat mass and body weight [15]. Here, we further measured body composition and fat distribution in 21-week-old male *Orm1*$^{+/+}$ and *Orm1*$^{-/-}$ mice using MRI. Representative coronal views were acquired by fat-selective whole-body imaging and showed that *Orm1*$^{-/-}$ mice had increased fat deposition in abdominal and subcutaneous areas compared to *Orm1*$^{+/+}$ mice (pseudocolor images from back to abdomen; adipose tissues: red and yellow; lean tissues and organs: blue) (Fig. 1a). Body composition analysis using a small animal body composition analyzer also showed a significant increase in fat mass in *Orm1*$^{-/-}$ mice compared to *Orm1*$^{+/+}$ mice (Fig. 1b). Furthermore, H&E staining showed that adipocyte size in the inguinal white adipose tissue (iWAT) of *Orm1*$^{-/-}$ mice was significantly larger than that of *Orm1*$^{+/+}$ mice (Fig. 1c, d).

In adipose tissue, fibronectin and collagens are the most prevalent ECM components, while LOX is an essential enzyme for collagen cross-linking and ECM mechanical properties. Our data showed that ORM1-deficient obese mice displayed increased Masson's trichrome staining (blue: collagen fibers) (Fig. 1c, e), as well as increased hydroxyproline (an amino acid specific to collagen) concentrations in iWAT (Fig. 1f), indicating excessive ECM deposition in adipose tissue. Accordingly, the expression of the fibrogenesis-related genes *Col1a1*, *Col3a1*, *Col6a3*, *Lox*, and fibronectin was also markedly increased (Fig. 1g–l). We also evaluated the expression of α-SMA, a well-recognized marker of myofibroblasts that is increased during fibrosis [18]. The results showed that *Orm1*$^{-/-}$ mice had higher α-SMA levels than *Orm1*$^{+/+}$ mice (Fig. 1g, h, m). These results suggested that ORM1 deficiency led to an obese phenotype with adiposity, excessive collagen deposition, and increased LOX-related collagen cross-linking indicating that endogenous ORM1 deficiency induced adipose tissue fibrosis.

ORM1 deficiency increases the expression of ECM regulators involved in adipose tissue fibrosis

ECM homeostasis is regulated by metalloproteinases (MMPs) and tissue inhibitors of metalloproteinases (TIMPs). MMPs are responsible for the degradation of ECM components, while specific TIMPs are able to inhibit MMP activity. Tissue fibrosis occurs as a consequence of the dysregulation of MMPs and TIMPs [8]. We further measured the mRNA expression of these ECM regulators in 21-week-old male *Orm1*$^{+/+}$ and *Orm1*$^{-/-}$ mice. The data showed that the mRNA expression of *Mmp-2*, *Mmp-13*, *Mmp-14*, *Timp-1*, *Timp-2*, and *Timp-3* was significantly increased in *Orm1*$^{-/-}$ mice compared to *Orm1*$^{+/+}$ mice (Fig. 2a, b). The corresponding protein expression, as assessed by immunoblotting, also showed a similar trend (Fig. 2c–i), suggesting a disturbance in ECM homeostasis and a metabolically unfavorable fat microenvironment.

ORM administration ameliorates the abnormal synthesis and degradation of ECM components in the iWAT of obese mice

The close relationship between ORM and fibrosis prompted us to consider whether exogenous ORM could alleviate adipose tissue fibrosis in obesity. We first examined the effect of purified ORM (50 mg/kg for 7 consecutive days) on HFD-induced obese mice. Compared with that in control mice, the mRNA expression of collagen (*Col1a1*, *Col3a1*, and *Col6a3*) in the iWAT of HFD mice was significantly increased, and this effect was attenuated by continuous ORM administration (Fig. 3a). Moreover, ORM also reduced the abnormal mRNA levels of the ECM regulators *Mmp-2*, *Mmp-13*, *Mmp-14*, *Timp-1*, *Timp-2*, and *Timp-3* in iWAT extracted from HFD mice (Fig. 3b, c). The protein levels of collagen and ECM regulators were further verified by Western blotting, and similar results were obtained (Fig. 3d–m). Furthermore, the mRNA and protein levels of α-SMA were also markedly increased in HFD mice and were reduced by ORM treatment (Fig. S1a–c).

In addition, we examined the effect of ORM on adipose tissue fibrosis in LepR-deficient *db/db* obese mice. The mRNA levels of collagen (*Col1a1*, *Col3a1,* and *Col6a3*) in the iWAT of *db/db* mice were significantly increased. Interestingly, only *Col6a3* overexpression was attenuated by ORM administration (Fig. 4a), while type VI collagen is the major collagen subtype in adipose tissue [19]. Moreover, the mRNA levels of the ECM regulators *Mmp-2*, *Mmp-13*, *Mmp-14*, *Timp-1*, *Timp-2*, and *Timp-3* were all significantly increased in iWAT extracted from *db/db* mice. However, only the increases in MMP-13 and TIMP-1 were attenuated by ORM treatment, while no significant changes were observed in the other ECM regulators (Fig. 4b, c). The protein levels of collagen VI, MMP-13, and TIMP-1 were further analyzed, and similar results were obtained (Fig. 4d–g). Further investigation of α-SMA showed that the mRNA and protein levels were increased in *db/db* mice and were reduced by ORM treatment (Fig. S1d–f).

ORM stimulates AMPK activity and inhibits TGF-β1 levels in the iWAT of obese mice

Tissue fibrosis is mainly mediated by TGF-β1, and activation of TGF-β1 signaling results in adipose tissue fibrosis in obese mice [8, 20]. Inhibiting TGF-β1 signaling is a major focus of antifibrotic therapy [7]. AMPK activation has been shown to alleviate fibrosis in different models, including renal and cardiac disease models [21–24]. Moreover, inhibiting TGF-β1-Smad3 signaling is one of the important downstream mechanisms by which AMPK alleviates adipose tissue fibrosis and ameliorates adipose tissue dysfunction [8, 25–27]. We previously reported that ORM could activate AMPK in skeletal muscle [28]. Therefore, we examined whether ORM could activate AMPK and inhibit TGF-β1 in adipose tissue. As shown in Fig. 5a–c, compared with those of control mice, both total and phosphorylated AMPK were reduced in the iWAT of HFD mice, while the expression of TGF-β1 was increased. ORM treatment increased both total and phosphorylated AMPK in the iWAT of HFD mice (Fig. 5a, b), and the expression of TGF-β1 was reduced (Fig. 5c). Similar results were obtained in *db/db* mice (Fig. 5d–f). Therefore, ORM stimulates AMPK activity and inhibits TGF-β1 in the adipose tissue of obese mice, which may contribute to alleviating adipose tissue fibrosis.

AMPK mediates the antifibrotic effect of ORM in vitro

To further investigate whether ORM ameliorates fibrosis by activating the AMPK pathway, 3T3-L1 fibroblasts were treated with TGF-β1 and used for in vitro experiments to establish an in vitro model simulating obesity-induced adipose fibrosis [8]. As shown in Fig. 6a–c, the mRNA expression of *Col1a1* and *Col6a3*

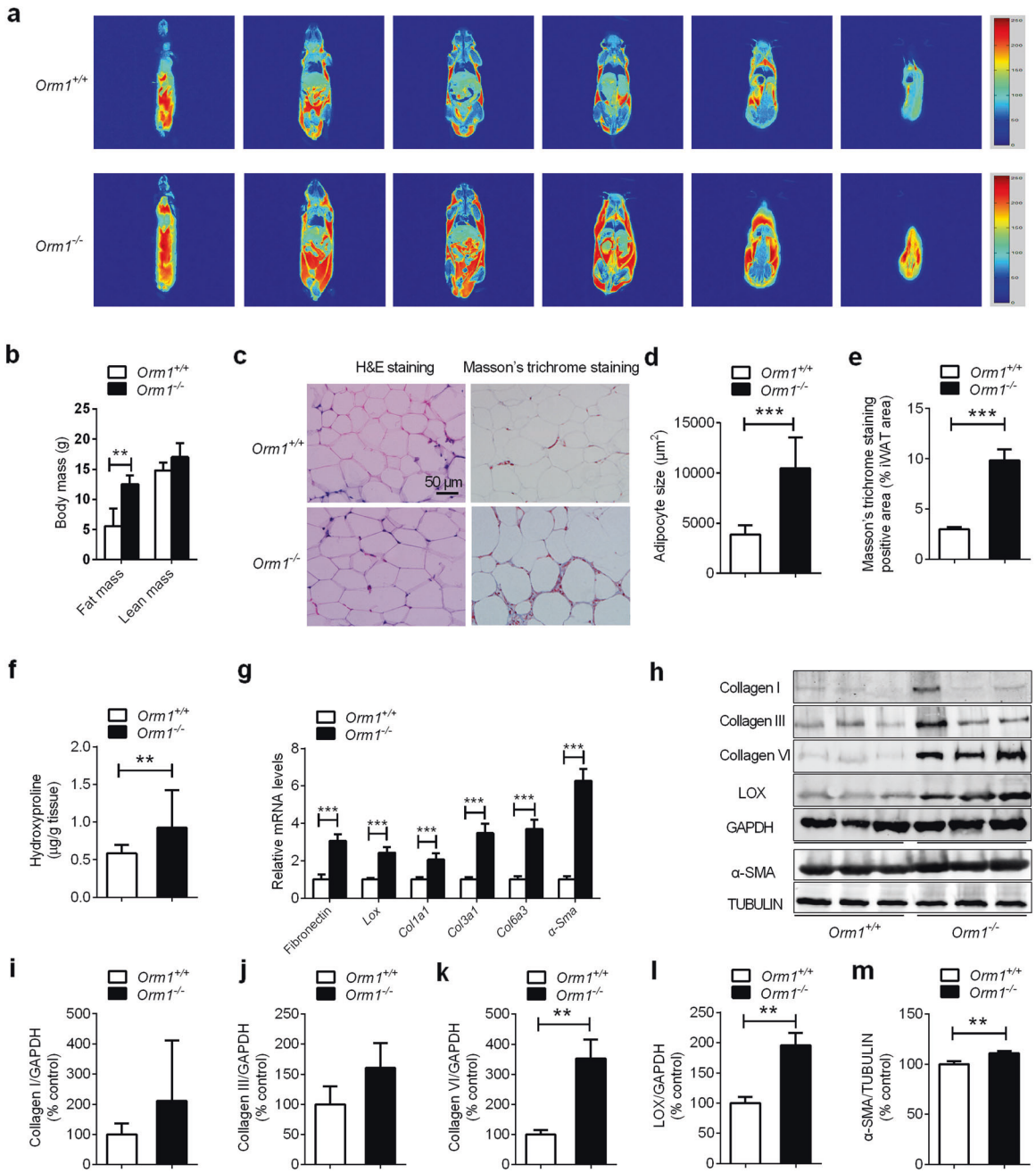

Fig. 1 ORM1-deficient mice exhibit an obese phenotype with adiposity and excessive collagen deposition. a Representative coronal views (from back to abdomen) of 21-week-old male *Orm1*$^{+/+}$ and *Orm1*$^{-/-}$ mice were acquired by fat-selective whole-body ^{1}H NMR pseudocolor images. Adipose tissues: red and yellow. Lean tissues and organs: blue. **b** Fat and lean body mass were quantified according to the MRI body composition analysis of the mice in **a** ($n = 3$ per group). **c** Representative H&E staining and Masson's trichrome staining of iWAT from 21-week-old male *Orm1*$^{+/+}$ and *Orm1*$^{-/-}$ mice. **d** The average adipocyte size in **c** ($n = 3$ per group). **e** The average Masson's trichrome stain-positive area (% iWAT area) in **c** ($n = 3$ per group). **f** The hydroxyproline levels in iWAT from 21-week-old male *Orm1*$^{+/+}$ and *Orm1*$^{-/-}$ mice ($n = 7$–8 per group). **g** Quantitative PCR analysis of fibrogenic genes encoding *Col1a1*, *Col3a1*, *Col6a3*, fibronectin, and *Lox* in iWAT. **h** Western blot analysis of iWAT extracted from 21-week-old male *Orm1*$^{+/+}$ and *Orm1*$^{-/-}$ mice ($n = 3$ per group). **i–m** Densitometric quantification of the data in **h**. *$P < 0.05$, **$P < 0.01$, ***$P < 0.001$ by Student's t test.

increased significantly after exposure to TGF-β1 for 24 h, and ORM treatment significantly reduced these levels. The mRNA expression of ECM regulators *Mmp-13* and *Timp-1* was also significantly elevated in 3T3-L1 cells exposed to TGF-β1, and this induction was largely reduced by ORM treatment (Fig. 6d, e). Then, the selective AMPK inhibitor dorsomorphin was used to verify whether AMPK mediated the antifibrotic effect of ORM. In the presence of dorsomorphin, all fibrotic markers tested were increased (Fig. 6a–f), and the inhibition of collagen overproduction by ORM was largely attenuated (Fig. 6a–c). Dorsomorphin also abolished the inhibitory effect of ORM on *Mmp-13* and *Timp-1* mRNA expression (Fig. 6d, e). In addition, LOX was associated with collagen fiber cross-linking. In accordance with the other indicators, ORM treatment inhibited LOX expression, and dorsomorphin reversed this effect (Fig. 6f–h). Similar results were observed in the expression of α-SMA (Fig. S2). Taken together with the results shown in Fig. 5, these results indicated that AMPK activation was involved in the regulation of ORM in adipose tissue fibrosis.

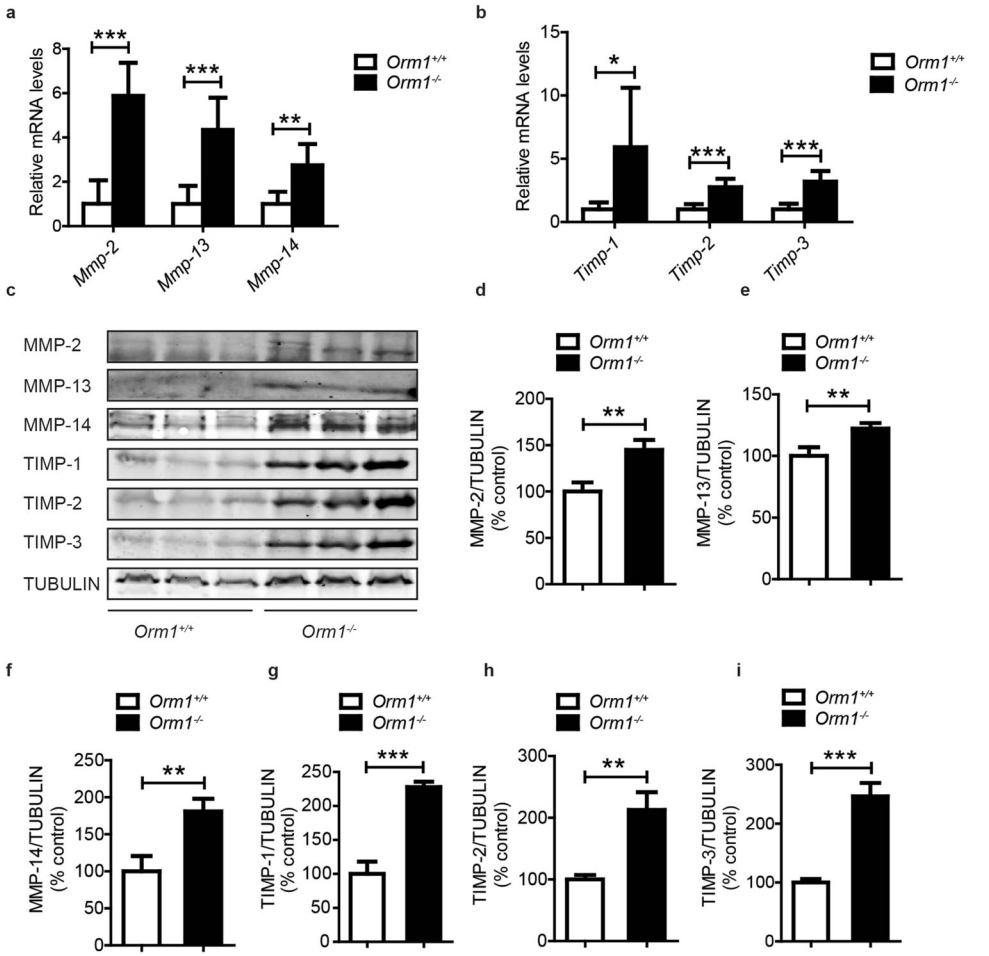

Fig. 2 ORM1 deficiency increases the expression of ECM regulators involved in adipose tissue fibrosis. a, b The mRNA levels of the ECM regulators *Mmp-2*, *Mmp-13*, *Mmp-14*, *Timp-1*, *Timp-2*, and *Timp-3* in iWAT extracted from 21-week-old male $Orm1^{+/+}$ and $Orm1^{-/-}$ mice ($n = 3$ per group). **c** Western blot analysis of iWAT extracted in **a** ($n = 3$ per group). **d–i** Densitometric quantification of the data in **c**. $^{*}P < 0.05$, $^{**}P < 0.01$, $^{***}P < 0.001$ by the Student's *t* test.

DISCUSSION

Antifibrotic therapies are crucial in preventing adipose tissue fibrosis and improving systemic metabolic dysregulation. Based on our previous study in which ORM1-deficient mice exhibited an obese phenotype, we further found that ORM1-deficient mice developed an adipose tissue fibrosis phenotype, while exogenous ORM administration could directly reverse this pathological process. Activation of the AMPK pathway and inhibition of TGF-β1 levels could mediate this protective effect (Fig. 7). Therefore, the adipocytokine ORM has been identified as a novel regulator of adipose tissue fibrosis and could be a novel therapeutic target.

Due to complex glycosylation, ORM has been reported to bind to several membrane receptors. ORM can act on LepR in the hypothalamus to control food intake [15], hemoglobin β-chain in hepatocytes to regulate its own uptake [29], and sialic acid binding immunoglobulin-like lectins (siglecs) in neutrophil granulocytes to induce increases in cytosolic Ca^{2+} [30, 31]. We also reported that ORM could bind C-C chemokine receptor type 5 (CCR5) in skeletal muscle to activate AMPK signaling [28]. Considering that ORM inhibits fibrosis in *db/db* mice, we strongly believe that CCR5, which is also expressed in adipose tissue, can mediate the effect of ORM on AMPK activation and fibrosis inhibition.

Dysfunction of ECM remodeling is the pathological basis of many diseases. In the case of adipose tissue, fibrosis occurs when the homeostasis between the synthesis and degradation of adipose tissue ECM proteins is disrupted and the ECM is excessively deposited. MMPs are zinc- and calcium-dependent proteases that promote the degradation of ECM components [32]. The activity of MMPs is mainly regulated by TIMPs, which can be divided into TIMP-1, TIMP-2, TIMP-3, and TIMP-4 [33]. In healthy tissue, the balance between TIMPs and MMPs controls the removal and assembly of ECM [34]. Although MMPs and TIMPs react in opposing manners, they are both highly induced under inflammatory and obesogenic conditions [35]. In our study, we found that ORM1 deficiency caused increased expression of MMP-2, MMP-13, MMP-14, TIMP-1, TIMP-2, and TIMP-3, indicating that the destruction of normal ECM and ECM remodeling promoted adipose tissue fibrosis. Thus, endogenous ORM is involved in maintaining the normal morphology and function of adipose tissue. Moreover, ORM treatment reduced the expression of ECM regulators and collagen in HFD mice and *db/db* mice (Figs. 3 and 4). Interestingly, all markers tested showed repressed expression in response to ORM treatment in HFD mice, but only MMP-13, TIMP-1, and type VI collagen were reduced by ORM treatment in LepR-deficient *db/db* mice. These data indicated that the leptin receptor could be essential in ORM-mediated regulation of certain fibrosis markers, which should be further explored. Thus, ORM may interfere with ECM remodeling by maintaining the balance between MMPs and

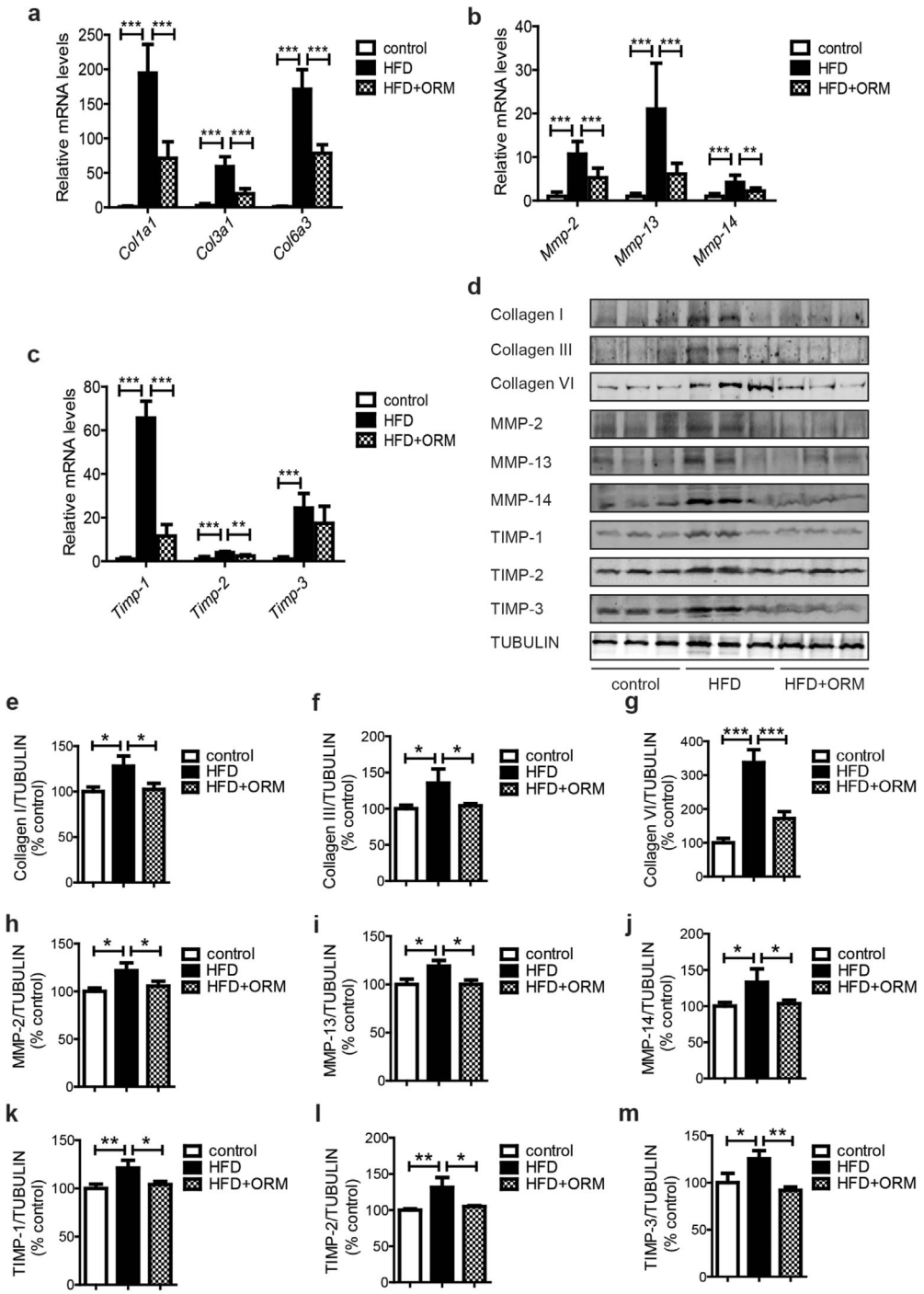

Fig. 3 ORM administration ameliorates the abnormal synthesis and degradation of ECM components in the iWAT of HFD mice. a The mRNA levels of *Col1a1*, *Col3a1*, and *Col6a3* in iWAT extracted from C57BL/6J mice fed a chow diet or 60% HFD (12 weeks) and treated with intraperitoneal injection of vehicle or 50 mg/kg ORM for 7 consecutive days ($n = 4$ per group). **b, c** The mRNA levels of the ECM regulators *Mmp-2*, *Mmp-13*, *Mmp-14*, *Timp-1*, *Timp-2*, and *Timp-3* in iWAT extracted from the mice in **a** ($n = 4$ per group). **d** Western blot analysis of iWAT extracted from the mice in **a** ($n = 3$ per group). **e–m** Densitometric quantification of the data in **d**. $^{*}P < 0.05$, $^{**}P < 0.01$, $^{***}P < 0.001$ by one-way ANOVA with the Tukey's test.

TIMPs, ultimately reducing collagen deposition, especially type VI collagen, which is the main ECM component in adipose tissue and forms the basal lamina surrounding adipocytes [5, 19, 36].

Normally, fibroblasts synthesize ECM. When fibrosis occurs, the ECM is mainly produced by myofibroblasts [18, 37]. Myofibroblasts are characterized by α-SMA expression, and the differentiation of these cells is a hallmark of fibrosis. Myofibroblast precursors vary in different tissues. In liver fibrosis, myofibroblasts are derived from hepatic stellate cells [18]. In pulmonary fibrosis, fibroblasts are the main source of myofibroblasts [18]. In adipose tissue fibrosis, myofibroblasts can differentiate from adipocytes, pre-adipocytes, macrophages, and mast cells [7], indicating a difference between adipose tissue and other tissues. In this study,

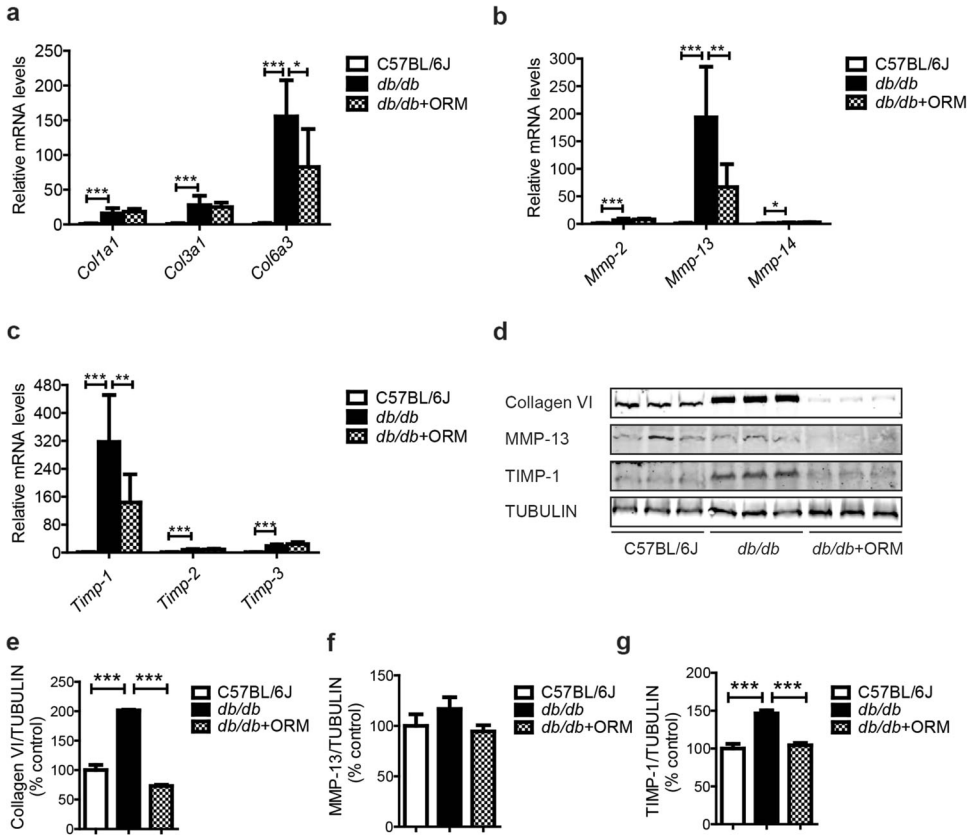

Fig. 4 ORM administration ameliorates the abnormal synthesis and degradation of ECM components in the iWAT of *db/db* mice. **a** The mRNA levels of *Col1a1*, *Col3a1*, and *Col6a3* in iWAT extracted from C57BL/6J mice and *db/db* mice treated with intraperitoneal injection of vehicle or 50 mg/kg ORM for 7 consecutive days ($n = 3$–4 per group). **b, c** The mRNA levels of the ECM regulators *Mmp-2*, *Mmp-13*, *Mmp-14*, *Timp-1*, *Timp-2*, and *Timp-3* in iWAT extracted from the mice in **a** ($n = 3$–4 per group). **d** Western blot analysis of iWAT extracted from the mice in **a** ($n = 3$ per group). **e**–**g** Densitometric quantification of the data in **d**. $^{*}P < 0.05$, $^{**}P < 0.01$, $^{***}P < 0.001$ by one-way ANOVA with the Tukey's test.

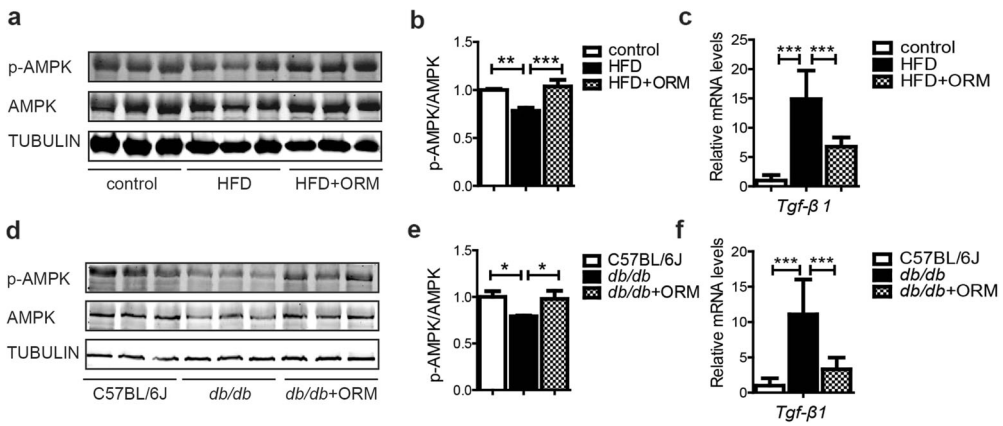

Fig. 5 ORM stimulates AMPK activity and inhibits TGF-β1 signaling in the iWAT of obese mice. **a** Western blot analysis of iWAT extracted from C57BL/6J mice fed a chow diet or 60% HFD (12 weeks) and treated with intraperitoneal injection of vehicle or 50 mg/kg ORM for 7 consecutive days ($n = 3$). **b** Densitometric quantification of the data in **a**. **c** The mRNA levels of *Tgf-β1* of iWAT extracted in **a** ($n = 4$). **d** Western blot analysis of iWAT extracted from C57BL/6J mice and *db/db* mice treated with intraperitoneal injection of vehicle or 50 mg/kg ORM for 7 consecutive days ($n = 3$). **e** Densitometric quantification of the data in **d**. **f** The mRNA levels of *Tgf-β1* of iWAT extracted in **d** ($n = 4$). $^{*}P < 0.05$, $^{**}P < 0.01$, $^{***}P < 0.001$ by one-way ANOVA with the Tukey's test.

we found that ORM could inhibit the abnormal expression of α-SMA in HFD-induced obese mice and *db/db* mice, as well as in TGF-β1-induced 3T3-L1 cells (Figs. S1 and S2), suggesting that ORM also plays an important role in inhibiting myofibroblast differentiation, which may also be a mechanism by which ORM inhibits fibrosis.

In addition, during adipose tissue expansion, hypoxia occurs and initiates fibrosis, which is further exacerbated by inflammation [7]. ORM is well known for its immunomodulatory effects [11, 12]. Whether the effect of ORM on adipose tissue fibrosis is related to its effect on inflammation and hypoxia remains to be further studied.

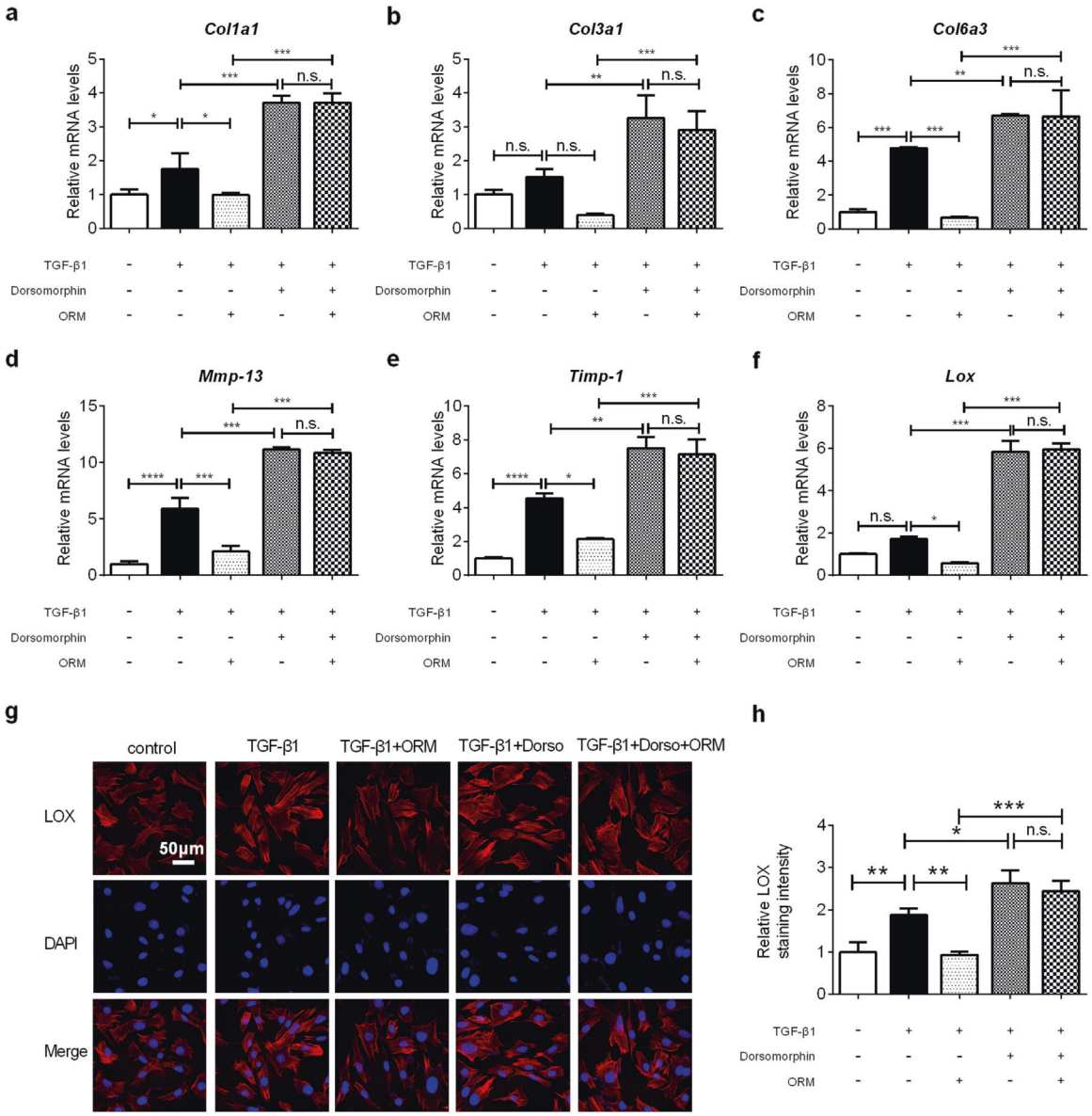

Fig. 6 AMPK mediates the antifibrotic effect of ORM in vitro. Relative mRNA levels of **a–c** collagen (*Col1a1*, *Col3a1*, and *Col6a3*), **d, e** ECM regulators (*Mmp-13* and *Timp-1*) and **f** the collagen fiber cross-linking marker *Lox* in 3T3-L1 cells treated with 5 ng/mL TGF-β1 for 24 h in the absence or presence of 10 μg/mL ORM and/or dorsomorphin (1 μmol/mL), as indicated ($n = 4$ per group). **g** Representative immunofluorescence images of the cells treated in **f**. **h** Quantification of LOX fluorescence shown in **g** ($n = 3$). $^{*}P < 0.05$, $^{**}P < 0.01$, $^{***}P < 0.001$ by one-way ANOVA with the Tukey's test.

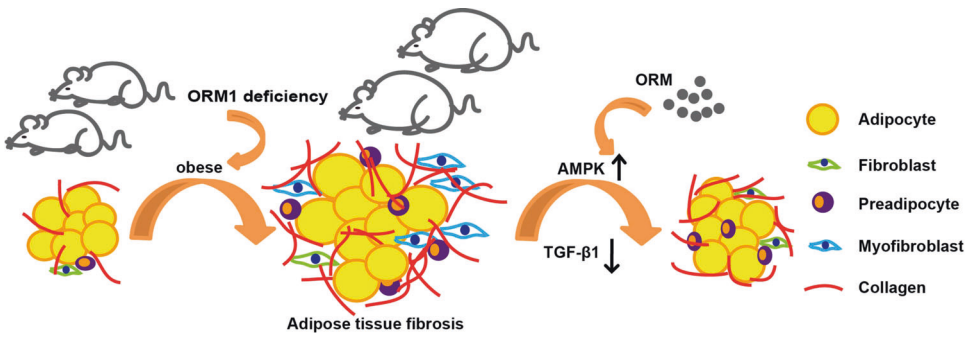

Fig. 7 Proposed mechanism by which ORM is involved in adipose tissue fibrosis. ORM1-deficient mice showed significant increases in fat mass and excessive collagen deposition. Exogenous administration of ORM activates adipose tissue AMPK, inhibits TGF-β1 levels, and reduces the expression of collagen and ECM mediators, thus alleviating adipose tissue fibrosis.

ACKNOWLEDGEMENTS

This study was supported by grants from the National Natural Science Foundation of China (Nos. 81773726, 82073907, and 82073842), the Shanghai Science and Technology Innovation Action Plan (Nos. 20ZR1470100, 18431900800, and 20S11902700), and the National Science & Technology Major Project "Key New Drug Creation and Manufacturing Program, China (No. 2018ZX09711002-003-015).

AUTHOR CONTRIBUTIONS

XL, YS, and PYW designed the study. XL, YS, and WDZ supervised the experiments. PYW and JYF carried out most of the experiments. ZZ, ZQ, YC, XMD, and BHH helped with some of the experiments. JW bred and maintained the ORM1-deficient mice. All authors analyzed and interpreted the experimental data. PYW and YS drafted the graphs and wrote the manuscript. XL revised the manuscript. ZZ and ZQ proofread and revised the manuscript.

ADDITIONAL INFORMATION

Supplementary information The online version contains supplementary material available at https://doi.org/10.1038/s41401-021-00666-9.

Competing interests: The authors declare no competing interests.

REFERENCES

1. Buechler C, Krautbauer S, Eisinger K. Adipose tissue fibrosis. World J Diabetes. 2015;6:548–53.
2. Chun TH. Peri-adipocyte ECM remodeling in obesity and adipose tissue fibrosis. Adipocyte. 2012;1:89–95.
3. Karsdal MA, Nielsen SH, Leeming DJ, Langholm LL, Nielsen MJ, Manon-Jensen T, et al. The good and the bad collagens of fibrosis—their role in signaling and organ function. Adv Drug Deliv Rev. 2017;121:43–56.
4. Guglielmi V, Cardellini M, Cinti F, Corgosinho F, Cardolini I, D'Adamo M, et al. Omental adipose tissue fibrosis and insulin resistance in severe obesity. Nutr Diabetes. 2015;5:e175.
5. Datta R, Podolsky MJ, Atabai K. Fat fibrosis: friend or foe? JCI Insight. 2018;3: e122289.
6. Lin D, Chun TH, Kang L. Adipose extracellular matrix remodelling in obesity and insulin resistance. Biochem Pharmacol. 2016;119:8–16.
7. Sun K, Tordjman J, Clément K, Scherer PE. Fibrosis and adipose tissue dysfunction. Cell Metab. 2013;18:470–77.
8. Luo T, Nocon A, Fry J, Sherban A, Rui X, Jiang B, et al. AMPK activation by metformin suppresses abnormal extracellular matrix remodeling in adipose tissue and ameliorates insulin resistance in obesity. Diabetes. 2016;65:2295–310.
9. Hasegawa Y, Ikeda K, Chen Y, Alba DL, Stifler D, Shinoda K, et al. Repression of adipose tissue fibrosis through a PRDM16-GTF2IRD1 complex improves systemic glucose homeostasis. Cell Metab. 2018;27:180–94.
10. Kawanishi N, Niihara H, Mizokami T, Yano H, Suzuki K. Exercise training attenuates adipose tissue fibrosis in diet-induced obese mice. Biochem Biophys Res Commun. 2013;440:774–9.
11. Fournier T, Medjoubi-N N, Porquet D. Alpha-1-acid glycoprotein. Biochim Biophys Acta. 2000;1482:157–71.
12. Luo Z, Lei H, Sun Y, Liu X, Su DF. Orosomucoid, an acute response protein with multiple modulating activities. J Physiol Biochem. 2015;71:329–40.
13. Lee YS, Choi JW, Hwang I, Lee JW, Lee JH, Kim AY, et al. Adipocytokine orosomucoid integrates inflammatory and metabolic signals to preserve energy homeostasis by resolving immoderate inflammation. J Biol Chem. 2010;285:22174–85.
14. Alfadda AA, Fatma S, Chishti MA, Al-Naami MY, Elawad R, Mendoza CD, et al. Orosomucoid serum concentrations and fat depot-specific mRNA and protein expression in humans. Mol Cells. 2012;33:35–41.
15. Sun Y, Yang Y, Qin Z, Cai J, Guo X, Tang Y, et al. The acute-phase protein orosomucoid regulates food intake and energy homeostasis via leptin receptor signaling pathway. Diabetes. 2016;65:1630–41.
16. Lei H, Sun Y, Luo Z, Yourek G, Gui H, Yang Y, et al. Fatigue-induced orosomucoid 1 acts on C-C chemokine receptor type 5 to enhance muscle endurance. Sci Rep. 2016;6:18839.
17. Dai B, Huang S, Deng Y. Modified insoluble dietary fibers in okara affect body composition, serum metabolic properties, and fatty acid profiles in mice fed high-fat diets: an NMR investigation. Food Res Int. 2019;116:1239–46.
18. Hinz B, Phan SH, Thannickal VJ, Galli A, Bochaton-Piallat ML, Gabbiani G. The myofibroblast: one function, multiple origins. Am J Pathol. 2007;170:1807–16.
19. Khan T, Muise ES, Iyengar P, Wang ZV, Chandalia M, Abate N, et al. Metabolic dysregulation and adipose tissue fibrosis: role of collagen VI. Mol Cell Biol. 2009;29:1575–91.
20. Meng XM, Nikolic-Paterson DJ, Lan HY. TGF-β: the master regulator of fibrosis. Nat Rev Nephrol. 2016;12:325–38.
21. Kim H, Moon SY, Kim JS, Baek CH, Kim M, Min JY, et al. Activation of AMP-activated protein kinase inhibits ER stress and renal fibrosis. Am J Physiol Ren Physiol. 2015;308:226–36.
22. Satriano J, Sharma K, Blantz RC, Deng A. Induction of AMPK activity corrects early pathophysiological alterations in the subtotal nephrectomy model of chronic kidney disease. Am J Physiol Ren Physiol. 2013;305:727–33.
23. Wang Y, Jia L, Hu Z, Entman ML, Mitch WE, Wang Y. AMP-activated protein kinase/myocardin-related transcription factor—a signaling regulates fibroblast activation and renal fibrosis. Kidney Int. 2018;93:81–94.
24. Qi H, Liu Y, Li S, Chen Y, Li L, Cao Y, et al. Activation of AMPK attenuated cardiac fibrosis by inhibiting CDK2 via p21/p27 and miR-29 family pathways in rats. Mol Ther Nucleic Acids. 2017;8:277–90.
25. Mishra R, Cool BL, Laderoute KR, Foretz M, Viollet B, Simonson MS. AMP-activated protein kinase inhibits transforming growth factor-beta-induced Smad3-dependent transcription and myofibroblast transdifferentiation. J Biol Chem. 2008;283:10461–9.
26. Li NS, Zou JR, Lin H, Ke R, He XL, Xiao L, et al. LKB1/AMPK inhibits TGF-beta1 production and the TGF-beta signaling pathway in breast cancer cells. Tumour Biol. 2016;37:8249–58.
27. Thakur S, Viswanadhapalli S, Kopp JB, Shi Q, Barnes JL, Block K, et al. Activation of AMP-activated protein kinase prevents TGF-beta1-induced epithelial-mesenchymal transition and myofibroblast activation. Am J Pathol. 2015;185:2168–80.
28. Qin Z, Wan JJ, Sun Y, Wang PY, Su DF, Lei H, et al. ORM promotes skeletal muscle glycogen accumulation via CCR5-activated AMPK pathway in mice. Front Pharmacol. 2016;7:302.
29. Komori H, Nishi K, Uehara N, Watanabe H, Shuto T, Suenaga A, et al. Characterization of hepatic cellular uptake of alpha1-acid glycoprotein (AGP), part 2: involvement of hemoglobin beta-chain on plasma membranes in the uptake of human AGP by liver parenchymal cells. J Pharm Sci. 2012;101:1607–15.
30. Atemezem A, Mbemba E, Vassy R, Slimani H, Saffar L, Gattegno L. Human alpha1-acid glycoprotein binds to CCR5 expressed on the plasma membrane of human primary macrophages. Biochem J. 2001;356:121–8.
31. Gunnarsson P, Levander L, Påhlsson P, Grenegård M. The acute-phase protein alpha 1-acid glycoprotein (AGP) induces rises in cytosolic Ca^{2+} in neutrophil granulocytes via sialic acid binding immunoglobulin-like lectins (siglecs). FASEB J. 2007;21:4059–69.
32. Nagase H, Woessner JF Jr. Matrix metalloproteinases. J Biol Chem. 1999;274:21491–4.
33. Brew K, Nagase H. The tissue inhibitors of metalloproteinases (TIMPs): an ancient family with structural and functional diversity. Biochim Biophys Acta. 2010;1803:55–71.
34. Roeb E. Matrix metalloproteinases and liver fibrosis (translational aspects). Matrix Biol. 2018;68-69:463–73.
35. Akama T, Chun TH. Transcription factor 21 (TCF21) promotes proinflammatory interleukin 6 expression and extracellular matrix remodeling in visceral adipose stem cells. J Biol Chem. 2018;293:6603–10.
36. Divoux A, Tordjman J, Lacasa D, Veyrie N, Hugol D, Aissat A, et al. Fibrosis in human adipose tissue: composition, distribution, and link with lipid metabolism and fat mass loss. Diabetes. 2010;59:2817–25.
37. Tomasek JJ, Gabbiani G, Hinz B, Chaponnier C, Brown RA. Myofibroblasts and mechano-regulation of connective tissue remodelling. Nat Rev Mol Cell Biol. 2002;3:349–63.